

Strength and Crack Growth Computation for Various types of Stringers for Stiffened Panels using XFEM Techniques

Krishna Lok S[†], Reshma G, Dattaguru B

[†]SID, CSIR-National Aerospace Laboratories, Bengaluru 560017, KA, India

Department of Aerospace Engineering, IIAEM-Jain University, Bengaluru 561112, KA, India

[†]E-mail: kls@nal.res.in

Abstract

In this paper the crack growth, modeling, and simulation of the stiffened and un-stiffened cracked panels presented using commercially available finite element software packages. Computation of stresses and convergence of stress intensity factor for single edge notch (SEN) specimens carried out using the finite element method (FEM) and extended finite element method (XFEM) and compared with an analytical solution. XFEM techniques like cohesive segment method and LEFM using virtual crack closure technique (VCCT), used for crack growth analysis and presented results for un-stiffened and stiffened panels considering various crack domain. The non-linear analysis considering both geometric and material non-linearity on stiffened panels with various stringers like a blade, L, inverted T and Z sections the results were presented. Arrived at the optimum stringer section type for the considered panel under axial loading from the numerical analysis.

Key Words: Key words SIF, XFEM, Crack growth, VCCT, Cohesive segment method

1. Introduction

This paper describes the crack growth, modeling and simulation using extended finite element techniques. Since the year 1940's, the aircraft fuselage design is mainly based on skin-riveted assemblies [1] and continued to use in aerospace vehicles for a foreseeable future. The development in technology has led to variations in a structural arrangement in the past several years. Over the years the main objective is towards the reduction in the number of rivets by reverting to bonded assembly or ideally manufacturing

separated components as an integrated structure for understanding the effects and growth of cracks.

In aircraft, construction stiffened plate structures have wide applications in the industry. They usually consist of the base structure and local reinforcement elements called stringers to improve the static and dynamic characteristics [2]. Stringer is a thin strip of stiffening member to which the skin of aircraft is fastened. They are primarily responsible for transferring the aerodynamic load acting on the skin to the frames and formers. Stiffeners also improve the strength and stability of the structure and provide means of slowing down the crack growth in the panel. Although riveted stringers act as crack stoppers several problems can arise such as locations of stress concentration leading to small cracks which may grow

Received: Oct. 13, 2018 Revised: Dec. 26, 2019 Accepted:
Dec. 28, 2019

[†] Corresponding Author

Tel: +91-80-2508-6977, E-mail: kls@nal.res.in

© The Society for Aerospace System Engineering

and extend through the complete section, spoiling the strength of the frame. The aim of this paper is to bring out the numerical methodologies to compute the behavior of integrally machined skin-stringer panels with a crack to study initiation and propagation process in fracture.

The standard FEM provides substantial advantages in solving with continuous field problems. However, for discontinuities, it is computationally expensive as mesh regenerated at each step. This disadvantage is overcome by an extended finite element method (XFEM). This paper describes the analysis of panels using the capabilities of XFEM. Structural panels for use in the manufacturing of fuselage panels and the effect of various stiffeners results are presented here.

2. Extended Finite Element Method

The eXtended Finite Element Method (XFEM) is a numerical method based on the Finite Element Method (FEM) specially designed for treating discontinuities (crack) and their growth. In order to model a crack with FEM, the geometry is explicitly represented by the mesh i.e. nodes placed across the crack and on the crack tip. Mesh refinement is necessary near the crack tips to represent the asymptotic fields associated with discontinuity. As the crack grows/propagates re-meshing becomes essential which is computationally expensive especially in complex geometries and 3D domains. Partition of unity (i.e. the sum of the shape functions must be equal to unity) concept is the mathematical background of XFEM [3]. It extends the classical FEM approach by enriching the solution space for solutions to differential equations with discontinuous functions.

In XFEM the discontinuity may not align with mesh i.e. the discontinuity is independent of mesh [4]. Hence for evolving discontinuities, frequent re-meshing is not required. XFEM allows discontinuities in an element by enriching degrees of freedom with special displacement functions. The discontinuity place is arbitrary with respect to the underlying finite element mesh and cracks propagation simulation performed without the need to re-mesh as crack advances. The XFEM based on enrichment of the FE model by adding extra degrees of freedom added to nodes of the elements cut by fracture. In this way, without modifying the domain discretization fracture being included in the numerical model as the mesh

completely independent of fracture. It is an attractive and effective way to simulate initiation and growth of a discrete crack along a definite path of real scenario in contrast to finite elements with continuous re-meshing and it does not need as many projections between the different meshes.

2.1 Interpolation scheme in XFEM

Approximation of XFEM consists of a standard finite element part i.e. the approximation of the FEM and the enrichments based on the idea of partition of unity approach [5]. Finite element interpolation or shape functions (N_i) also, satisfy the partition of unity condition. By taking advantage of this property it is possible to enrich the finite element approximation space as given in Eq. (1).

$$u(x) = \underbrace{\sum_{i=1}^n N_i(x)u_i}_{\text{classical}} + \underbrace{\sum_{i=1}^n N_i(x) \sum_{j=1}^k p_j a_{ij}}_{\text{enriched}} \quad (1)$$

where N_i is standard FE function for node i , p_j is the enrichment functions, u_i is the finite element degrees of freedom associated with the continuous part of approximation and a_{ij} is the extra degrees of freedom associated with the discontinuous part of the approximation. Fracture mechanics is essentially formulated to deal with strong discontinuities (cracks) where both the displacement and strain fields are discontinuous across a crack surface as in Eq. (2).

Continuity equations:

$$\text{Displacement (u) strain } (\epsilon): u^+ + u^- = 0 \ \& \ \epsilon^+ + \epsilon^- = 0$$

$$\text{Weak discontinuity: } u^+ + u^- = 0 \ \& \ \epsilon^+ + \epsilon^- \neq 0 \quad (2)$$

$$\text{Strong discontinuity: } u^+ + u^- \neq 0 \ \& \ \epsilon^+ + \epsilon^- \neq 0$$

2.2 Crack enrichment functions

Heaviside enrichment [6] is a typical enrichment function considered for crack. The common practice is to incorporate two enrichment functions into the XFEM displacement approximation to represent a crack. The generalized Heaviside step function is used to model the interior of crack. The Heaviside $H(x)$ is given by Eq. (3)

$$H(x) = \begin{cases} 1, & \text{above crack} \\ -1, & \text{below crack} \end{cases} \quad (3)$$

For those elements that are cut by crack, the displacement is enriched by multiplying the Heaviside step function by nodal enriched degrees of freedom. The crack tip is modeled using crack-tip enrichment function which incorporates radial and angular behaviour of two-dimensional asymptotic crack-tip displacement field [7]. The crack tip enrichment functions in isotropic elasticity are given by Eq. (4)

$$a_i(r, \theta) = \left\{ \sqrt{r} \sin\left(\frac{\theta}{2}\right); \sqrt{r} \cos\left(\frac{\theta}{2}\right); \sqrt{r} \sin\left(\frac{\theta}{2}\right) \sin \theta; \sqrt{r} \cos\left(\frac{\theta}{2}\right) \sin \theta \right\} \quad (4)$$

where, r and θ are polar co-ordinates in the local crack-tip co-ordinate system. The origin is at the tip and $\theta = 0$ is parallel to the crack.

The crack growth considered unstable or stable or neutral when the energy at equilibrium is a minimum or maximum or zero respectively. A sufficient condition for crack stability is obtained from the second derivative of $(\Pi + U_\Gamma)$, Eq. (5):

$$\frac{\partial^2 (\Pi + U_\Gamma)}{\partial a^2} \begin{cases} < 0 & \text{unstable fracture} \\ = 0 & \text{stable fracture} \\ > 0 & \text{neutral equilibrium} \end{cases} \quad (5)$$

3. Problem Formulation

The numerical solution activity started with a stationary crack and further continued with crack growth simulation. In our problem 6061-T6 aluminum is chosen as the material for analysis on a Single Edge Notch (SEN) specimen. The material properties [8] used in this analysis being shown in Table 1. The width 'w' is 225mm height 'h' is 450mm thickness is unity and 'a' being crack length varying from 22.5mm to 90mm. Uni-axial pressure of 5MPa or displacement of 5mm being applied at top edge in the y-direction and fixed at bottom edge for pure mode I analysis as shown in Fig. (1a). The second problem of a panel included a stringer. All the thickness as 2mm constant maintained for various stringers and panel. The other dimensions for various stringers are as indicated in Figures 2a, 2b, 2c, and 2d, all are not to scale.

Variation of stresses in y-direction around crack-tip for isotropic linear elastic material⁸ in mode I is shown in Fig. (1b). This variation of stress is expressed as in Eq. (6)

$$\sigma_{yy} = \frac{K}{\sqrt{2\pi r}} \cos \frac{\theta}{2} \left[1 + \sin \frac{\theta}{2} \sin \frac{3\theta}{2} \right] \quad (6)$$

where, r is the distance away from the crack tip and θ is the orientation of that point from crack tip. On the crack plane $\theta = 0$. Therefore

$$\sigma_{yy} = \frac{K}{\sqrt{2\pi r}} \quad (7)$$

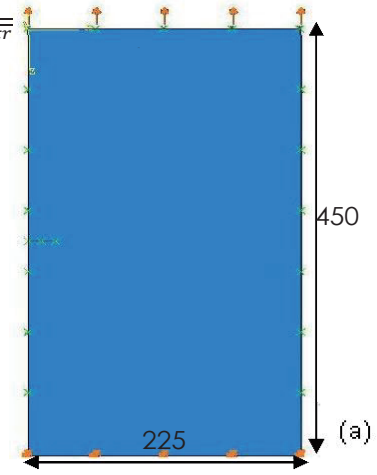
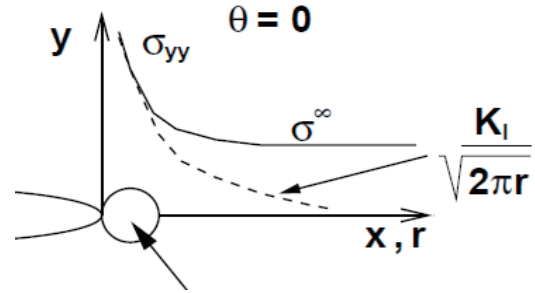


Fig. 1. (a) Geometry, Boundary conditions, and Enriched domain

(b)



Singularity Dominated Zone

Fig. 1 b Stress normal to crack plane in mode I

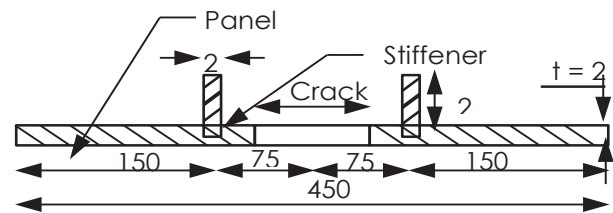


Fig. 2a. Cross sectional view of blade (straight) stringer with the panel

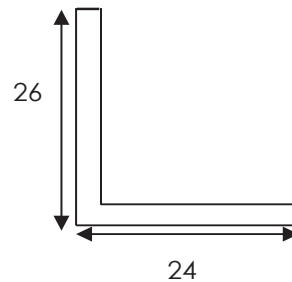
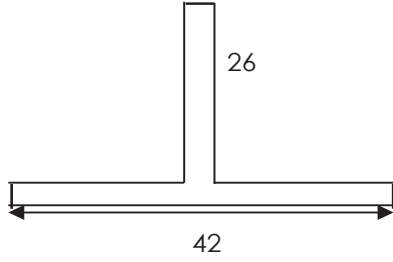
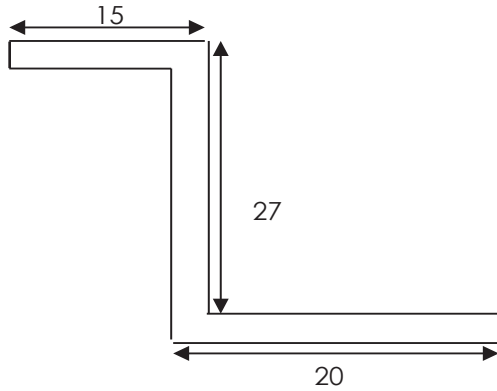


Fig. 2b Cross sectional view of L Stringer**Fig. 2c** Cross sectional view of inverted T stringer**Fig. 2d** Cross sectional view of Z stringer**Table 1.** Material and its strength properties

Young's Modulus (E)	Poisson's Ratio (ν)	Maximum Principal Stress	Intensity Factor (K _I)	Critical Stress Energy Release Rate (G _I C)
70GPa	0.33	146.3MPa	24 MPa (m) ^{1/2}	24.2kJ/m

3.1 Stress intensity factor

The Stress Intensity Factor (SIF) is an important parameter in a cracked structure for estimating the severity of the crack. SIF characterizes the stresses, strains, and displacements near the crack tip and its calculation is limited to linear elastic fracture mechanics [9]. The analytical solution of edge crack on the rectangular plate under tensile loading [10] is given by Eq. (8) $K_I =$

$$\sigma \sqrt{\pi a} F\left(\frac{a}{w}\right)$$

(8)

The geometric function $F\left(\frac{a}{w}\right)$ is from empirical formula [11]

$$F\left(\frac{a}{w}\right) = 1.122 - 0.231\left(\frac{a}{w}\right) + 10.550\left(\frac{a}{w}\right)^2 - 21.710\left(\frac{a}{w}\right)^3 + 30.382\left(\frac{a}{w}\right)^4 \quad (9)$$

The stress computation near the crack tip region for different crack length a to width ratio a/w (0.1, 0.2, 0.3 and 0.4) was carried out. Stress intensity factor values from different crack lengths are computed using 3D XFEM (C3D8R), 2D FEM (CPS4R) and 3D FEM (C3D8R) analytically as shown in Table 2. SIF values of FEM 2D and FEM 3D are closer to values of that obtained by empirical relation. XFEM 3D has shown higher results with a deviation of less than 4%. Table 3 shows the tabulation of SIF values obtained from FEM 2D for $a/w = 0.1$. It depicts the mesh convergence with an increase in mesh density.

Table 2. Comparison of SIF values for mode I analysis

a/w	K _I		K _I XFEM 3D	K _I empirical	Shape factor F(a/w)
	K _I FEM2D	K _I FEM 3D			
0.1	49.53	50.82	53.9	50.69	1.206
0.2	80.67	83.04	87.55	83.05	1.397
0.3	120.1	123.7	130.2	124.12	1.705
0.4	176.7	181.8	191.4	183.53	2.183

Table 3. Tabulation of SIF values for mode I analysis on FEM 2D

Serial	Number of nodes	K _I (MPa√mm)	Element size(w*h)
1	863	46.12	20*40
2	3325	45.95	40*80
3	13049	45.88	80*160
4	51697	45.88	160*320

4. Methodology

Crack growth simulation mainly consists of 3 steps crack initiation, crack propagation and failure. All these steps, simulated using XFEM elements in ABAQUS without any re-meshing near the crack tip. The numerical analysis code used is the ABAQUS – Standard. It provides two approaches for studying the initiation and propagation of crack-using XFEM.

4.1 XFEM based Linear Elastic Fracture Mechanics

Linear Elastic Fracture Mechanics (LEFM) is the fundamental theory for crack/fracture, initially developed by Griffith and versatile theory that deals with sharp cracks in elastic bodies. The Virtual Crack Closure Technique (VCCT) criterion uses the principles of LEFM and so for crack propagation problems of brittle material. It provides the effective means to predict the onset of crack growth by calculating the strain energy release rate associated with a crack. A pre-existing crack is explicitly included in the finite element mesh. The key assumption is that the energy released by extending the crack by length Δa is equal to the work required to close the crack over the length Δa [12, 13]. In general, a case involving mode I, mode II and mode III the fracture criterion being defined as in Eq. (10)

$$f = \frac{G_{equiv}}{G_{equivC}} \geq 1 \quad (10)$$

where, G_{equiv} the strain energy release rate is calculated at a node and G_{equivC} is the critical strain energy release rate calculated based on user-defined mode-mix criterion reaches the value of 1.0.

4.2 XFEM based Cohesive segment method

The cohesive segment approach [14,15] is used to simulate fracture initiation and propagation and is based on cohesive elements or on surface-based cohesive behaviour. In this method fracture initiation and propagation, simulated along an arbitrary path in materials. Using this approach, the near-tip singularity is not required and only the displacement jump function across an element is considered. Therefore, the fracture has to propagate across an entire element at a time to avoid the need to model the stress singularity.

Maximum principal stress criterion used for initiation of crack. It is expressed as shown in Eq. (11),

$$f = \left\{ \frac{\langle \sigma_{max} \rangle}{\sigma_{max}^o} \right\} \quad (11)$$

where σ_{max}^o represents the maximum allowable principal stress. The Macaulay brackets $\langle \sigma_{max} \rangle$ are used to signify that purely compressive stress state does not initiate damage ($\langle \sigma_{max} \rangle = 0$ if $\sigma_{max} < 0$ and $\langle \sigma_{max} \rangle = \sigma_{max}$ if $\sigma_{max} \geq 0$) the damage initiates when Maxps ratio reaches a value of unity i.e. $f = 1$. An additional crack length of an existing crack is extended after an equilibrium increment when the

fracture criterion, f , reaches the value 1.0 within a given tolerance f_{tol} .

$$1.0 \leq f \leq 1.0 + f_{tol}$$

If $f \geq 1 + f_{tol}$ the time increment is cut back such that the crack initiation criterion is satisfied. In this study, the value of f_{tol} is 0.05.

5. Results and Discussions

A three-dimensional panel considered to determine the crack path and simulate crack growth. Initial crack is created using the shell. An aluminum material of 6061-T6 panel 450mm length, 450mm width, thickness as 2mm and a crack length of 22.5mm is considered for analysis as shown in Fig. (2a). Only half of the panel with one stiffener is modelled due to geometric symmetry. Displacement of 1mm (GN analysis) and 5mm (MN & GN analysis) being applied at the top and bottom edge for all the panel analyses. Various stiffeners like a blade (straight), L, inverted T, and Z were used for analysis on the stiffened panels replicating real experimental scenarios. An optimum mesh was selected for meshing the model i.e. 8-noded hexahedral 7776 element, reduced integration, hourglass control (C3D8R) and 24108 nodes.

A metallic panel is modelled as a linear (elastic) or elastoplastic depending on the requirement. However, the actual behaviour will be elastoplastic in an experiment and in reality. In order to simulate non-linearity (plastic behaviour) of the material, true stress-strain [16,17] values input in the model for analysis. The True stress-strain [16] data given in table 4 used in the model for analysis.

The crack growth models are modelled with geometric nonlinearity to cater for larger displacements as the crack grows. The top edge of the panel selected to obtain load-displacement curves. The load-displacement curves obtained for both unstiffened and blade type stiffened panels results presented in figure 3a. The reaction force here represents the load carried by the panel. In an analysis involving both geometric and material non-linearity wherein plasticity is invoked the load displacements plots are given in figure 3b. In comparison with GN alone and GN-MN together there is a difference of about 100N.

Table 4 True Stress-Strain Data

Stress (MPa)	True Plastic Strain
--------------	---------------------

111.0	0.0
112.6	0.0019
113.6	0.0038
116.1	0.0067
116.9	0.0086
118.7	0.0135
120.7	0.0183
122.5	0.0231
124.6	0.0279
127.5	0.0326
130.0	0.0421
133.3	0.0514
136.1	0.0607
139.3	0.0699
141.8	0.0790
144.4	0.0881
146.3	0.0971

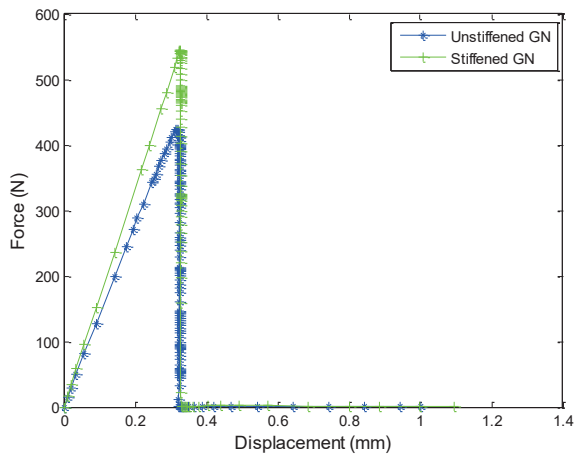


Fig. 3(a) Geometric Non-linear (GN) only

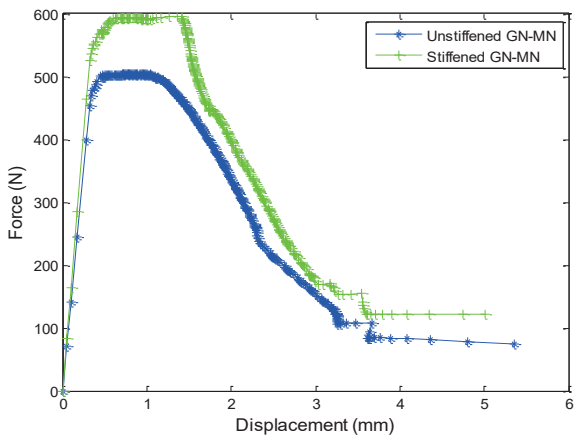


Fig. 3(b) GN and Material Non-linear simulation plots

The simulation carried out with the whole panel as an enriched region i.e. the full panel considered as the crack domain where crack propagates. Similarly, only a part of a panel near the crack region was enriched in which crack propagates as shown in figure 4a.

The load-displacement plots for full and partial enrichment on the elastic panel using both XFEM techniques is shown in figure 4b. It is observed that partial enrichment has no effect on the solution. Unnecessary use of computational resources avoided.

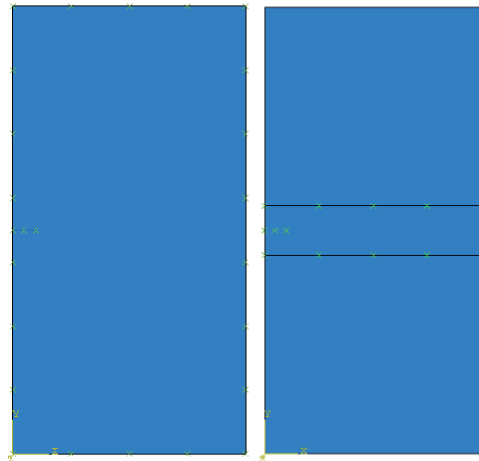


Fig. 4 (a) XFEM model showing partial and full enrichment represented by light green colour cross marks

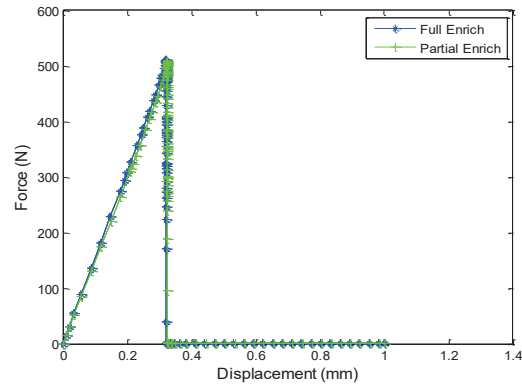


Fig. 4(b) Load-displacement curves for partial and full enrichment using XFEM results

In the case of a stiffened panel XFEM based cohesive segment method, used as it renders good results for ductile materials. Two cases are studied, one with crack domain only in panel, stiffener not getting cracked and other with panel and stiffener both modelled as crack domains. The load-displacement curve for the unstiffened panel was compared with a blade (straight) type stiffened panel with both crack domain results shown in figure 5a. It is observed that

the stiffened panel carries a 15% extra load than an un-stiffened panel considering both skin and stringer as a crack domain.

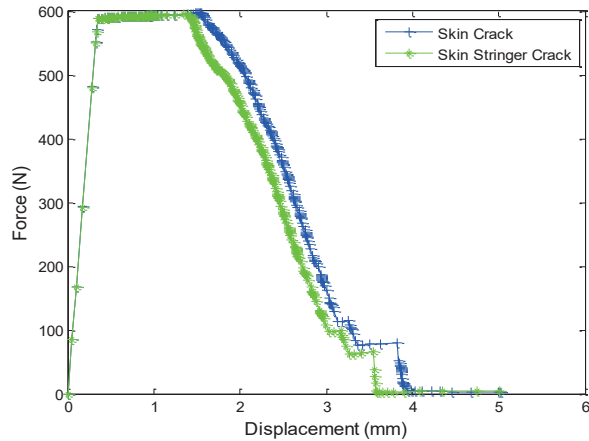


Fig. 5 (a) Load-displacement curves for stiffened panel with different crack domains

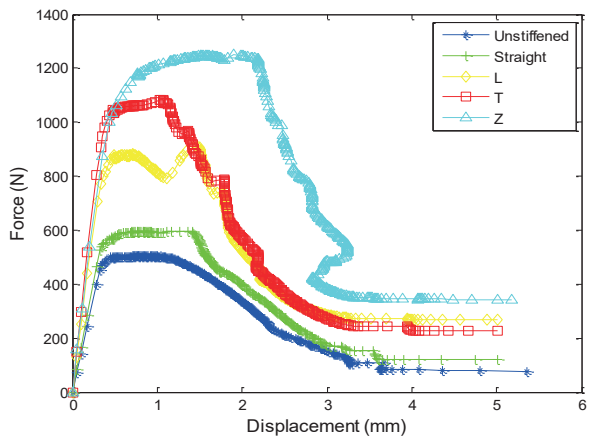


Fig. 5 (b) Load-displacement curves for un-stiffened and various stringers on stiffened panel

Various stringers like a blade (straight), L, inverted T, and Z are considered for analysis with dimensions as shown in Fig. (2) with both skin and stringer as the crack domain by invoking both geometry and material nonlinearity models. In this work, we have not considered an I-section stiffener. I-stiffeners have manufacturing difficulties. The aim of this work is to design for manufacturing and simulate realistic cases. The plots obtained shown in Figure 5b. It's observed un-stiffened panel carries the least load also model fails earliest. In the case of stiffeners with an increase in the material, there is an increase in stiffness and load-carrying capacity of the panel. L and inverted T stiffened panel have the same plastic zone region, however, inverted T stiffener predicts higher load than L stiffener. Z stiffened panel shows highest

plastic zone & predicts very slow crack growth and highest load compared to other stringers. Figure 6a shows the crack initiation stress magnitudes and figure 6b the level-set value (PHILSM) across the panel. Table 4 gives strength computation of various stringers on the stiffened panel at crack initiation point Load carrying capacity of stiffened panel with each type of stringer in comparison with the un-stiffened panel being obtained i.e., L stiffened panel 44%, inverted T stiffened panel 50% and Z stiffened panel 59% higher load than unstiffened panel.

Table 4 Strength computation of various stringers

Variables	Un-stiffened	Blade	L	Inverted T	Z
Von mises (N/mm ²)	124.6	125.4	125.8	128.9	131.3
Reaction force (N)	502	591.2	993.2	1056	1246
Displacement (mm)	0.475	0.495	0.468	0.473	0.86
PHILSM	2.778	2.778	2.778	2.778	2.778
Strength (%) (compared to un-stiffened panel)	-	15	44	50	59

6. Concluding Remarks

In this paper, systematic computation, carried out for various stress components, SIF and crack growth simulation considering various stringers and results being presented with increasing complexity. The linear computed stress parameters around crack tips are as expected and XFEM 3D has rendered higher stresses than finite element method. SIF values for different meshes showing mesh convergence were presented and compared with theoretical values which show a percentage deviation of 4%. The case with stiffener not getting cracked with only skin as crack domain provides the highest load as stiffener resists the deformation applied.

The crack growth simulation was done on an un-stiffened panel using both XFEM techniques, XFEM based LEFM (using VCCT) and XFEM based cohesive segment method case, both techniques are in good agreement.

The simulation carried out on stiffened and un-stiffened panel considering different crack domains, has shown no effect on the maximum load-carrying capacity. The stiffened panel has shown 15% higher strength than the un-stiffened panel.

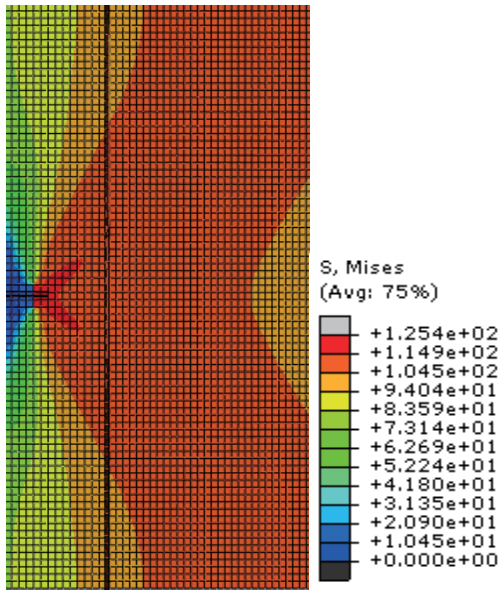


Fig. 6 (a) Stress contour at the start of crack initiation

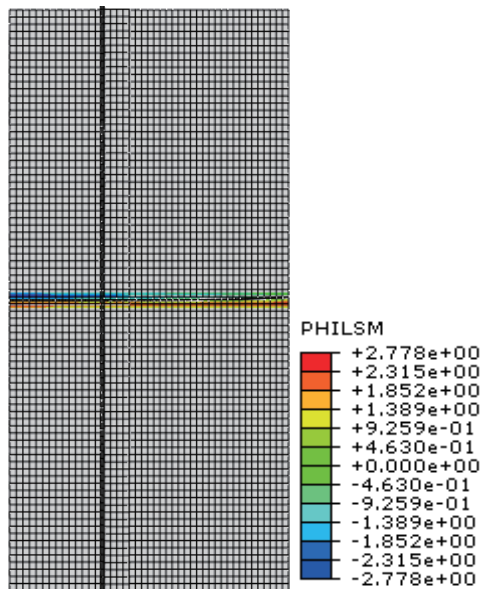


Fig. 6 (b) Variation of PHILSM along the length of the panel

Crack growth simulated on the stiffened panel-based cohesive segment method as it provides better

results for ductile material, using blade, L, Inverted T and Z stringers and strength results were tabulated. Optimum stringer selected in case of both skin-stringer as a crack domain for geometric and material non-linear analysis. Z stiffener predicts the highest load (59%) than the un-stiffened panel. Also, it shows the highest plastic zone indicating strength and deformation it would resist. It shows very slow crack growth. Based on these observations selection of Z type stringer under uniaxial loading would be an ideal case.

Acknowledgments

The authors thank the Director, CSIR-National Aerospace Laboratories, and Dr Satish Chandra, Head, STTD for their kind support and guidance rendered throughout the activity. Authors also thank all those who have contributed directly or indirectly in presenting this work in the present form.

References

- [1] Fossati M., Colombo D., Manes A., and Giglio M., "Numerical modelling of crack growth profiles in integral skin-stringer panels", *Eng Fract Mech*, 78(2011) 1341-1352
- [2] Ali Yeilaghi Tamijani, Rakesh K. Kapania, "Vibration of plate with curvilinear stiffeners using mesh-free method", *AIAA Journal*, Vol 48, (8), August 2010, DOI: 10.2514/1.43082
- [3] Krishna Lok Singh, Kamal Keswani, and Mallikarjun Vaggar, "Crack growth simulation of stiffened panels using XFEM techniques", *Indian Journal of Engineering & Materials Sciences*, Vol. 21, Aug. 2014, pp. 418-428.
- [4] Soheil Mohammadi, "Extended Finite Element Method for Fracture Analysis of Structures", 2008, Blackwell Publishing Ltd.
- [5] E. Giner, N. Sukumar, J. E. Tarancon, F. J. Fuenmayor, "An abaqus implementation of the extended finite element method", *Eng Fract Mech*, 2008
- [6] N. Sukumar, J. H. Prevost, "Modeling quasi static crack growth with the extended finite element method", *International Journal of solids and structures* 40(2003) 7513-7537
- [7] Safdar Abbas, Alaska Alizada, Thomas-Peter Fries, "Mode-independent approaches for the XFEM in fracture mechanics", *Int. J. Numer. Meth. Engng* 2010

- [8] Matthew J. Pai, Nam-Ho Kim, “Modeling Failure in Composite Materials with the Extended Finite Element and Level Set Methods”, 50th *AIAA/ASME/ASCE/AHS/ASC Structures, Structural Dynamics and Material Conference* May 2009
- [9] Anderson T. L., *Fracture Mechanics: fundamentals and applications*, 2nd ed, (CRC Press, USA) ISBN 0-8493-4260-0(1994)
- [10] George E. Blandford, Anthony R. Ingraffea, James A. Liggett, “Two-dimensional stress intensity factor computations using the boundary element method”, *International Journal for Numerical Methods in Engineering*, Vol 17, 387-404(1981)
- [11] Abaqus 6.xx, Analysis User’s Manual volume number II, Analysis procedures and solution (2011).
- [12] Palani G. S., Nagesh R. Iyer, and B. Dattaguru, “Fracture Analysis of Stiffened Panels Under Combined Tensile, Bending, and Shear Loads”, *AIAA Journal*, Vol. 43 (9), September 2005.
- [13] Sundararajan Natarajan, D. Roy Mahapatra, Stephane P. A. Bordas, “Integrating strong and weak discontinuities without integration subcells and example applications in an XFEM/GFEM framework”, *International Journal for Numerical Methods in Engineering*, Vol 83 (3), 269-294, 2010 DOI: 10.1002/nme.2798
- [14] Tada H., Paris P. C. & Irwin G. R., *The stress analysis of cracks handbook*, 3rd ed, (Professional Engineering Publishing), 2000
- [15] Ronald Krueger, “Virtual crack closure technique: History, approach and applications”, *Appl Mech Rev* Vol 57 (2), March 2004
- [16] Remmers J. J. C., Needleman A., “A cohesive segments method for simulation of crack growth”, *Computational mechanics* 31(2003) 69-7, Springer Verlag 200, DOI 10.1007/s00466-002-094-z
- [17] Reinhardt L. & Cordes J. A., *XFEM Modeling of Mixed-Mode Cracks in Thin Aluminum Panels*, SIMULIA customer conference, 2010.